TRANSPORT
ISSN 1648-4142 / eISSN 1648-3480
2022 Volume 37 Issue 4: 291–309
https://doi.org/10.3846/transport.2022.17067

RELIABLE PLANNING OF HINTERLAND-PORT FREIGHT NETWORK AGAINST TRANSFER DISRUPTION RISKS

Lei WANG[1], Qing LIU[1,2*]

[1]*School of Transportation and Logistics Engineering, Wuhan University of Technology, China*
[2]*National Engineering Research Center for Water Transport Safety, Wuhan University of Technology, China*

Submitted 12 April 2019; resubmitted 14 September 2019, 26 October 2019; accepted 8 November 2019

Abstract. Many previous cases have shown that port operations are susceptible to disruptive events. This paper proposes 2-stage Stochastic Programming (SP) for port users to reliably plan the hinterland-port intermodal freight network with consideration of risk aversion in cost. Probabilistic disruptions of intermodal terminals are considered as scenario-specific. In the 1st stage, intermodal paths are selected to obtain proper network capacities. In the 2nd stage, cargo flows are assigned for each disruption scenario on the planed network. The 2-stage model is firstly formulated in a risk-neutral environment to achieve the minimum expectation of total cost. Then, the Mean-Risk (MR) framework is adopted by incorporating a risk measure tool called Conditional Value-at-Risk (CVaR) into the expectation model, so as to reduce the cost of worst-case disruption scenarios. Benders' Decomposition (BD) is introduced to efficiently solve the exponential many problem. Some numerical experiments are performed under different risk aversion parameters. With this study, network planners can decide network capacities with reasonable redundancies to improve the freight reliability in a cost-effective way. The proposed method provides a simple approach for the planners to quantify their risk appetites in cost and to impose them in the planning process, hence to trade-off the Expected Cost (EC) and the worst-case cost.

Keywords: hinterland-port freight, reliable planning, disruption risks, 2-stage stochastic programming, conditional value-at-risk, Benders' decomposition.

Notations

BD – Benders' decomposition;
BBD – basic BD;
BnB – branch and bound;
BnC – branch and cut;
CPU – central processing unit;
CVaR – conditional VaR;
EC – expected cost;
HPFN – hinterland-port freight network;
IT – information technology;
MIP – mixed integer programming;
MR – mean-risk;
NP – non-deterministic polynomial;
O–D – origin–destination;
SP – stochastic programming;
VaR – value-at-risk.

Introduction

Ports as the interface of water-land transportations and value adding activities play an indispensable role in international trade. In China, for example, a recent statistics bulletin on transportation industry development issued by the Ministry of Transport states that, nearly 4 billion tons of the annual inbound and outbound cargos are transhipped at over 27000 public-use sea and inland berths (MoT 2017). With the expansion of operation complexity and scope, ports are vulnerable to ubiquitous disruptive events, arising from malicious attacks, accidents, operational disorders or natural catastrophes, etc. In 2017, category 4 hurricane Harvey made landfall in the US and most of the ports along Gulf of Mexico were hence shut down due to severe damages or inundations of structures (Blake, Zelinsky 2017). The 2010 Chile earthquake triggered significant facility failures in 10% of the coastal nation's industrial ports concentrated in a region close to the

*Corresponding author. E-mail: *lqwhutjt@whut.edu.cn*

epicentre (Brunet *et al.* 2012). Apart from contingencies, intended activities, e.g., the long-term port labour strike on the US west coast in 2014 (ISSConline 2014), are also able to make the services, operations and transfer of cargos out of balance. The impacts of such unforeseen situations may propagate far along the whole transportation network (Miller-Hooks *et al.* 2009).

Areas served by a port are referred to its hinterland, over which port users, including all types of shippers and receivers, choose the port as the transfer connection on water-land intermodal paths and coordinate and oversee the entire cargo delivering process on the paths (Wang *et al.* 2016). Hinterland areas, alternative ports, O–D pairs and potential intermodal paths constitute a spatially distributed system, which is called the HPFN herein. Due to the discontinuities of transportation operations after detrimental events, network users may be under direct financial pressures in the form of delays in cargo delivery, supply shortages and reassignment of cargo flows to substituting facilities requiring higher costs (Dixit *et al.* 2016). Therefore, port users need to take into account the disruption risks of ports in the planning phase for more reliable cargo transfer process, so as to maintain the freight continuity with a best cost efficiency.

The expectation is a common and simple criterion for decision-making under uncertainties (Filippi *et al.* 2017). Adopting the expectation criterion aims at optimizing the average transportation performance on the network system. In worst-case, the arising of high-impact disruptions can lead to premium expenses owing to severe losses, which is not simply the financial pressure but can be critical challenges in business competitiveness for port users. However, the optimization of the EC is often unable to account for desirable worst-case costs (Sawik 2011). That means it is sometimes crucial to achieve both of them at the same time in the HPFN planning.

Massive research efforts related to port safety management still focus on risk identification and assessment or countermeasure formulation in individual ports or berths (Emecen Kara 2016; John *et al.* 2014; Yang *et al.* 2014). Those works are the basics of understanding the probabilistically evolving process of hazardous events, while neglecting the interdependence of components in the transport process. A handful of studies are appearing on holistically managing port disruptions, which sorely evaluate or qualitatively cope with the impacts on port-based business chain (Novati *et al.* 2015). Works on transportation planning associated with port-related freight network under disruption risks are still insufficient, e.g., Chen *et al.* (2017) developed a model to optimize the resilience of the hinterland-port transportation, while the network is based on a single port; Lewis *et al.* (2013) studied the inventory strategy of supply chains facing port disruption risks.

In the domain of general transportation network planning, decision-makers share an increasing ardency of finding the most efficient approaches to reduce the effects of unconventional events. One stream of the works pays attention to pre-event planning or immediate post-event actions for best performance of emergency responses or recoveries (Chen, Miller-Hooks 2012; Dixit *et al.* 2016; Huang *et al.* 2007; Miller-Hooks *et al.* 2012; Mohaymany, Pirnazar 2007;). Another stream of the researches focuses on hardening the in-operation network with the implementation of protecting measures ahead of disruptions (Fan *et al.* 2010; Liu *et al.* 2009; Lu *et al.* 2018).

Both of the above 2 kinds of works pursue the best network capacity or the minimal cost with a concern on public interests rather than from the view of logistics or transport operators. A 3rd stream of the studies is called reliable planning (Snyder, Daskin 2005), which allows logistics or transport operators to consider additional network capabilities against disruptions according to their own needs. One of the earliest models was given by Drezner (1987), who introduced the concept of reliable facility location to a *p*-median system. A number of papers coping with random hazardous factors have significantly extended the mathematical formulation and application range of the reliable location model (Cui *et al.* 2010; Li *et al.* 2013; Snyder and Daskin 2005; Yu *et al.* 2017). The main idea of those works is that, once there are facilities out of service, the capability redundancy planned at the very beginning can immediately and seamlessly back up a part of or even all the cargo delivery.

On the sector of reliable planning, SP is an useful approach to model changing and uncertain situations in the planning period (Cui *et al.* 2010; Yu *et al.* 2017). It allows freight managers to trade-off the initial set up cost and the recourse cost, including the day-to-day operation cost and the loss from the unavailability of facilities. Most of the relevant works are still scenario-specific, that is, possible disruption situations are identified with discrete scenarios (Carturan *et al.* 2013; Marufuzzaman *et al.* 2014). The recourse cost under a facility location decision is then easily expressed with an expectation subject to a set of discrete probabilistic parameters determined by the decision and all potential disruption realizations.

Another major trade-off is between the expectation and the risk when the risk-averse attitude of the decision-maker is considered. The risk herein means the uncertainty in cost caused by the volatility of disruption degrees, such as the abovementioned extreme losses in worst-cases. That trade-off can be accomplished by adopting the MR framework that incorporates risk measurements into the risk-neutral model (Gotoh, Takano 2007; Lu *et al.* 2018).

Several risk measure tools in the domain of financial engineering, like the variance, mean absolute deviation or VaR, have been carried out and applied in the field of portfolio management over the past decades. As an alternative of VaR, by far a standard tool of risk management (Xu *et al.* 2016), most recently CVaR is obtaining its popularity due to its superior properties in aspect of conformity to the coherent axiom and preservation of convexity. That tool has been involved in various areas, such as portfolio

investment (Chen, Yang 2017; Xu *et al.* 2016), supplier and order managing (Sawik 2011, 2013b), crop cultivating (Filippi *et al.* 2017), energy scheduling (Tan *et al.* 2017), IT security planning (Sawik 2013a) and hazardous material freighting (Faghih-Roohi *et al.* 2016). CVaR is represented by the tail mean or the worst-case expectation. The optimization of CVaR is in company with the compute of the VaR (Uryasev 2000; Rockafellar, Uryasev 2000), which is the quantile decided by a given confidence level. It seeks for what exact magnitude the downside investment returns exceeding the VaR could be lessen to. The planning of uncertain transportation network embedding CVaR can lay a hedge around extreme scenarios costs (Lei *et al.* 2018; Liu *et al.* 2009; Lu *et al.* 2018).

In addition, a wide range of disruption realizations will result in massive scenario-related flow assignment variables. With the presence of integer facility location variables, the deterministic equivalent of the SP problems can be MIP in large size. The general solution frameworks for MIPs are established on BnB or BnC that runs BnB while employs cutting planes to tighten relaxations (Jünger *et al.* 2010), and both of them are always time-consuming and may run out of memory when the problem scale is large. So far, extensive algorithmic efforts on decomposition approaches have been made for specific transportation problems. BD (Cordeau *et al.* 2001) was frequently applied to solve scenario-specific transportation models (Chen, Miller-Hooks 2012; Marufuzzaman *et al.* 2014; De Camargo *et al.* 2008), which can take advantage of the *block-ladder* structure of scenario-specific problems. It progressively narrows the restriction of the problem with small number of Benders' cuts hence is performed in a computational cheaper manner (Chen, Miller-Hooks 2012).

To summarize the similarities and differences of the abovementioned literature, comparisons of their main features in aspect of research object, scope and main focus, are presented in Table 1. Relevant work review reveals that there is an absence of multi-port based freight network planning from the perspective of port users to prevent the impacts of disaster events at the very beginning of network facility location. This paper aims to fill the research gaps by introducing the concept of reliable planning into the HPFN issues and by proposing a decision-making approach for port users to holistically organize the freight process against port disruptions with capacity redundancies in a cost-effective way. The problem will be formulated as scenario-based 2-stage stochastic MIPs in both a risk-neutral and a risk-averse environment. BD algorithm that is common used in scenario-based problems is adopted for faster solving.

The reminder of this paper is as follows: in Section 1, the description of the reliable planning for the HPFN is provided; Section 2 formulates the risk-neutral and the risk-averse optimizations MIPs; BD algorithm is presented in Section 3; Section 4 is the computational examples; some conclusions are given at the last section.

Table 1. Key features of relevant studies

Object	Scope	Main focus	Sources
Individual ports	Port safety or security management	Risk identification and assessment or countermeasure formulation	Emecen Kara (2016); John *et al.* (2014); Yang *et al.* (2014)
Port based supply chains	Business chain risk management	Investigation of the role of ports in supply chain disruptions	Novati *et al.* (2015)
Port based supply chains	Inventory risk reduction of customers	Supply ordering strategy formulation under port-of-entry disruptions	Lewis *et al.* (2013)
Freight networks based on single port	Emergency management from the view of shippers	Recovery activity selection following disruptions	Chen *et al.* (2017)
General freight and traffic networks	Emergency management for public interests	Response or recovery activity selection following disruptions	Chen, Miller-Hooks (2012); Dixit *et al.* (2016); Huang *et al.* (2007); Miller-Hooks *et al.* (2012); Mohaymany, Pirnazar (2007)
General traffic networks	Disaster prevention for public interests	Infrastructure protection activity selection ahead of disruptions	Fan *et al.* (2010); Liu *et al.* (2009); Lu *et al.* (2018)
General supply chain networks	Disaster prevention from the view of logistics operators	Reliable design against disruptions at the very beginning of logistics facility location with capacity redundancy	Cui *et al.* (2010); Drezner (1987); Li *et al.* (2013); Snyder, Daskin (2005); Yu *et al.* (2017)
General freight, traffic and supply chain networks	Considering risk aversion in network planning under uncertainty	Integration of the CVaR tool to hedge the highest potential costs	Faghih-Roohi *et al.* (2016); Lei *et al.* (2018); Liu *et al.* (2009); Lu *et al.* (2018); Yu *et al.* (2017)

1. Problem description

1.1. HPFN planning

An HPFN consists of a intermediate port region and its landward hinterland and seaward hinterland. The landward hinterland is divided into several discontinuous demand areas, each of which includes certain port users who operate intermodal freights on the network. It is assumed that the freight process of each demand area originates from/ends at a hub station in the area, which functions like a dry port (Chen *et al.* 2017) and serves all the port users in the demand area. Each hub station is able to link with all the terminals in the intermediate port region by land transportation modes, including rail or road. There is a set of oversea ports in the seaward hinterland, and transportation routes between the transfer terminal and the oversea port are coastal or ocean waterways. Inbound/outbound cargos of port users are delivered between the demand areas and the oversea ports (called O–D pairs) and are transferred at the intermediate terminals.

Although there may be several physical and geographical routes linking a demand area and a terminal, those routes are simply represented as a single and capacity-based land link for the following reasons. 1st, the selection of the land link between a demand area and a terminal represents the situation that the port users in the demand area will use the freight paths that pass through the terminal, rather than make the choice of specific routes; 2nd, since the demand areas are discontinuous, no cargo between a demand area and the terminal will be connected by the hub station in any other demand areas; at last, the disruption is only associated with the transfer terminals, which will not spread to the land link infrastructures, and the capacities of them will keep stable. Therefore, the detailed transport network topology in the landward hinterland is out of discussion in this paper.

At the seaward hinterland side, vessels normally can as well as need to be dispatched amongst terminals or oversea ports to optimize the cabin utilization, so the capacities of the water links are often deemed as unbounded. Nevertheless, there can be some special water links like the fixed shipping lines, which still have certain capacity limitations.

With the above analyses and assumptions, we can depict the structure of the HPFN for our case as Figure 1.

Planning of the HPFN is from the perspective of port users in the landward hinterland, because it aims to determine how the given network resources can be utilized to maximize their interests rather than how the resources can be provided. For a relatively long-term running, suppose the port users can cooperate with each other to share the expenses and there is a common agency serves and directs them in aspect of intermodal path selection and cargo flow assignment on the paths at the system level.

An O–D pair can be linked by different intermodal paths that use different terminals, so the choices of paths are in company with the choices of terminals. Due to the

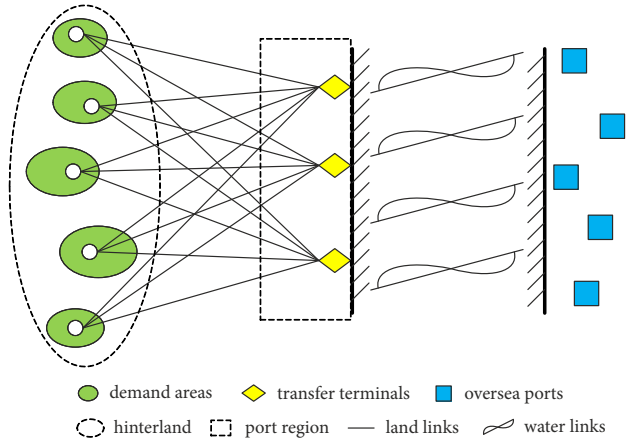

Figure 1. A sample of the HPFN

difference of size between conveyances, cargos transported by truck or train on land links are organized in relatively small amounts, while vessels on water links often depart from or arrive at terminals with larger stowage. That means cargo batches need to be reassembled and reloaded at the transfer terminals. So, to select a terminal, the agency needs to order from the terminal manager both the reloading service supply and a place to temporarily store cargos that wait for vehicles or vessels.

Besides, the running of intermodal paths should be supported by connection offices, which are normally set in the scope of the selected terminals to coordinate the on-site transfer procedure, like transhipment scheduling, custom clearance and commodity inspection. The agency can allocate the connection office by terminal, by path or by demand area. For the 1st case, only one office will be set in each selected terminal, handling all the paths passing through the terminal, which can be a cheap but less efficient way. For the 2nd case, a series of offices will be set in each selected terminal, and each of them connects a specific intermodal path passing through the terminal to maximize the transfer rate, but it can be quite costly. For the last case, in each selected terminal there are also several offices, while the number of them is less than that in the 2nd case, and each serves only the paths between a certain demand area and all the related oversea ports. Considering both cost and efficiency, we adopt the last case in this study, and in so doing, with the allocation of a connection office, the land link between the corresponding demand area and terminal is decided.

The costs of the terminal ordering and the connection setting constitute the fixed cost. Another part of the total cost is the variable cost, decided by the flow assignment on the planned network. As for the flow assignment on transportation networks, 2 important principles are found in literature: user equilibrium or system optimization. The former works well when network users can continuously gather information like charge, travel time and path capacity and are able to adjust the flow assignment according to those real-time network status. The network users are treated independently and cannot benefit from merely

changing their own routing decisions in equilibrium condition. Since theories of modelling individual routing behaviours still need more practicability validations (Fan, Liu 2010), the system optimization principle, which holds that all flow assignments are also under centralized directing and control, is adopted in this paper, by which we can estimate a lower bound that the cargo flow cost is possible to achieve at the system level (Liu *et al.* 2009).

When elements like freight demands and network capacity keep stable, the planning of the HPFN is a normal facility location problem for minimal overall value of the fixed cost and the variable cost. However, in a changing environment, especially following unconventional events such as earthquake, hurricane, flood, labour strike or economic crisis, port operations can be disrupted for a time. As a consequence, terminal capacities may decrease in the planning period. Therefore, the variable cost should count both the cargo travel cost and the loss from unsatisfied freight demands.

Whether all the freight demands in the planning period can be totally satisfied under disruption conditions reflects if the network is absolutely reliable for the freight, and how many of the demands are satisfied represents the degree of freight reliability. Since we always use a large value as a "penalty cost" to impact the loss in the variable cost (Lu *et al.* 2018), once there are unsatisfied demands the variable cost will increase, and the magnitude of the variable cost is decided by the loss from unsatisfied freight demands. Therefore, the distribution of the variable cost indicates the state of freight reliability in a general meaning. One of the most direct and effective way in reliable planning is the preparedness of transfer capacity redundancy, aiming to improve freight reliability with reasonable cost efficiency.

1.2. Research framework

The reliable planning of the HPFN is based on the identification of probabilistic disruption scenarios, so the problem is formulated with stochastic optimization. The planning process is divided into 2-stages, where the firtsly stage is to select paths ahead of potential disaster emerging and the 2nd stage assigns cargo flows on the decided network for each disruption scenario. The optimization firstly takes the expected overall freight cost as the decision criterion, which is a risk-neutral decision-making. Then, the CVaR tool, focusing on the high-impact and low-probability scenarios, is incorporated into the above risk-neutral model in succession to consider the risk aversion of decision-makers, hence the optimization is performed with the trade-off between the expectation and the tail mean of the overall cost.

In Figure 2, the research framework is divided into 5 steps. After the abovementioned modelling of stochastic 2-stage optimization, a BD algorithm for model solution is proposed, and then the models and the solving method are validated by some computational examples.

2. Formulations of 2-stage SP

The following formulations are on the basis of some general assumptions: demands of O–D pairs are predictable in a certain period; the variable cost of transport and transfer does not count differences in goods and transport modes; disasters emerging in the port region will not spread to links, namely the transport supply of land and water links are assumed to be intact; the freight system is formulated as a undirected network, where the capacities of links and nodes are shared in 2 directions including both the inbound and outbound freight. Meanwhile, input

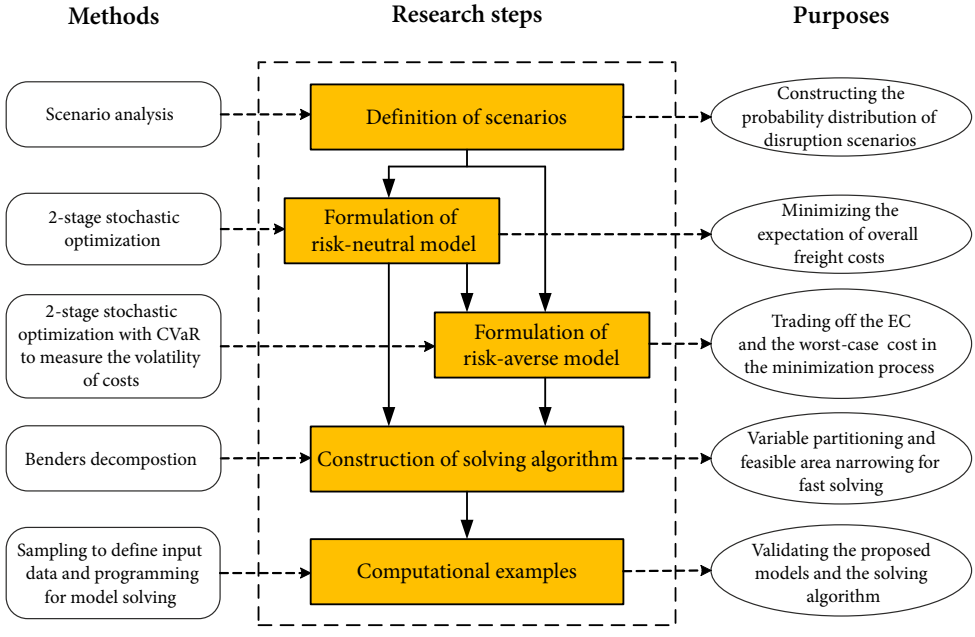

Figure 2. The flow chart of the research contents

parameters like transportation demands, capacity decline ratios and probabilities of disasters or disruptions are statically defined over a whole period. Consequently, the flow assignments for scenarios will be figured out with overall values, which are not further discussed among different time intervals on the planning horizon. A set of notations for the following discussions is given in Table 2.

2.1. Probabilities of disruption scenarios

For a certain terminal, the disruption probability is prepared by synthesizing the probabilities of disaster events in the port region and the following damages to the terminal operations, while the 2 sets of probabilities are often not readily available in practice. Over a given planning period, the occurring probability of all kind of events able to cause disruptions in the port cluster can be predicted by statistical analysing with historical data. Under the given disaster situation, the probability of damage to each terminal needs to be estimated one by one. Since faced with insufficiency of objective data, the damage probability is hard and time-consuming to estimate rigorously. Inference techniques based on knowledge and experiences, which are popular in safety management, like event chain analysis, fuzzy logic system, evidential reasoning or Bayesian network, can be employed to obtain the damage probabilities with experts' help.

Suppose $J_\xi \subseteq J$ is a subset of terminals from the alternative set which are damaged after the disaster situation, then it defines a disruption scenario ξ. For simplicity, the damage level of a terminal only considers binary states, where: 1 – indicates being damaged; 0 – otherwise. We can express the disruption scenario probability as:

Table 2. Notations

Sets	
I	demand areas in the landward hinterland, indexed by i
J	alternative terminals in the port region, indexed by j
K	oversea ports, indexed by k
W	O–D pairs between node i and node k, indexed by $w(i, k)$, $i \in I$, $k \in K$
Ξ	disruption scenarios, indexed by ξ
Parameters	
c_j	maximal transfer capacity supply of terminal j for the port users
a_{ij}	maximal transport capacity supply on land link between demand area i and terminal j for the port users
a_{jk}	maximal transport capacity supply on water link between terminal j and oversea port k for the port users
d^w	freight demand of O–D pair w, where $D = \sum_{w \in W} d^w$ represents the total demands
q_j^w	unit transport cost for O–D pair w on the path passing through terminal j
g_j	unit transfer cost at terminal j, including storing, displacement handling and reloading cost
t_{ij}	setup cost of connecting agency for port users at area i to use paths passing through terminal j
h_j	ordering cost of terminal j
l^w	loss from an unit of unsatisfied demand of O–D pair w, which can be estimated by freight charges, liquidated damages and consequential social and economic impacts
τ	probability of disasters in port region over the planning period
p_j	probability of terminal j being disrupted by the occurred events, which are supposed to be site-dependent
δ_j	expected rate of declined capacity of terminal j in the planning period, based on the estimation of disruption duration, where $\delta_j \in [0,1]$
$P(\xi)$	probability of disruption scenario ξ
$\delta_j(\xi)$	expected rate of declined capacity for terminal j under disruption scenario ξ in the planning period, where $\delta_j(\xi) \in [0,1]$
B	budget for fixed cost
θ	confidence level
Decision variables	
x_j	0–1 variable indicating whether or not terminal j is selected
y_{ij}	0–1 variable indicating whether or not a connection office is opened for the paths using the land link between demand area i and terminal j
$u_j^w(\xi)$	fraction of total demand of O–D pair w transhipped at terminal j under scenario ξ
α	VaR of total transportation costs
$T(\xi)$	relaxation variable for the difference between cost of tail scenario ξ and VaR

$$P(\xi)=\text{prob}\left[J_\xi\right]=\begin{cases}\tau\cdot\prod_{j\in J_\xi}p_j\cdot\prod_{j\notin J_\xi}\left(1-p_j\right), & J_\xi\neq\phi;\\ \left(1-\tau\right)+\tau\cdot\prod_{j\in J}\left(1-p_j\right), & J_\xi=\phi,\end{cases}\quad(1)$$

where: $\sum_{\xi\in\Xi}P(\xi)=1$; the universal set Ξ is the power set of J, i.e., if there are L terminals, the number of possible scenarios is 2^L; each disruption scenario ξ and its probability $P(\xi)$ link with a set of capacity decline rates associated with the alternative terminals $\Delta(\xi)=\left\{\delta_j(\xi)\middle|j\in J\right\}$, where $\delta_j(\xi)=\delta_j$ if $j\in J_\xi$, otherwise $\delta_j(\xi)=0$.

The binary expression of damage level simplifies our discussion. Nevertheless, for each terminal, damage can be classified into several levels, ranging from no damage to complete breakdown, and the probabilities associated with the damage states are represented with a discrete set. In so doing, the disruption scenario can be defined as a subset of terminals in certain damage states. Once probabilistic data are sufficient for more detailed discussion, the disruption scenario probability can be conveniently extended to cases with more damage states, without revisions of its structure. If necessary, it will be more typical to consider broader sets of damage levels in practice, which often leads to more accurate optimization outcomes, while the number of the disruption scenarios will increase rapidly with the growth of damage levels. Moreover, when the above random parameters fit continuous distributions, Monte Carlo sampling can facilitate generating manageable number of discrete scenarios (Liu *et al.* 2009).

2.2. Risk-neutral decision-making

The mean value of total costs is used to measure the average quality of a decision in a risk-neutral environment. Let $C_\xi=f_\xi(\boldsymbol{x},\boldsymbol{y})$ be the total cost for scenario ξ, which is the sum of the cost to select terminals and paths $\sum_{j\in J}x_j\cdot h_j+\sum_{i\in I}\sum_{j\in J}y_{ij}\cdot t_{ij}$ and the recourse cost $H_\xi(\boldsymbol{x},\boldsymbol{y})$. Each cost C_ξ is corresponding to a probability $P(\xi)$. With the above descriptions, the risk-neutral optimization is represented as a 2-stage stochastic MIP as below.

2-stage EC:

1st stage:

$$\min E\left(C_\xi\right)=\min_{\boldsymbol{x},\boldsymbol{y}}\sum_{j\in J}x_j\cdot h_j+\sum_{i\in I}\sum_{j\in J}y_{ij}\cdot t_{ij}+\sum_{\xi\in\Xi}P(\xi)\cdot H_\xi(\boldsymbol{x},\boldsymbol{y})\quad(2)$$

subject to:

»» terminal and path selection constraints:

» each terminal used by any opened path should be selected;

» each selected terminal is passed by paths opened for at least one demand area:

$$\frac{1}{R}\cdot\sum_{i\in I}y_{ij}\le x_j,\ \forall j\in J;\quad(3)$$

$$x_j\le\sum_{i\in I}y_{ij},\ \forall j\in J,\quad(4)$$

where: R is the number of demand areas; the combination of constraint (3) and (4) makes the selection of a terminal and the opening of one or more connections in the terminal are in company with each other, so the paths are available and the selected terminal is in use;

»» budget constraints:

» budget constraint for fixed costs:

$$\sum_{j\in J}x_j\cdot h_j+\sum_{i\in I}\sum_{j\in J}y_{ij}\cdot t_{ij}\le B,\quad(5)$$

where: constraint (Equation (5)) means that the model pursuits risk reduction with reasonable rather than unlimited backup capacities, hence to avoid possible high wastes of redundant capacities and unbearable initial setup cost. Note that excessively low budget sometimes results in infeasible solutions if the planned network capacity fails to completely satisfy the demands, so the limitation should be carefully set;

»» binary constraints:

$$x_j\in\left\{0,1\right\},\ \forall j\in J;\quad(6)$$

$$y_{ij}\in\left\{0,1\right\},\ \forall i\in I,\ \forall j\in J.\quad(7)$$

In the above 1st stage model Equations (2)–(7), $H_\xi(\boldsymbol{x},\boldsymbol{y})$ is a minimized variable cost determined by both the 1st stage decision and the particular scenario realization ξ, which comprises the cargo travel cost and the loss, if any, from the transfer capacity shortages. For each scenario, the recourse function can be stated as the following 2nd stage problem.

2nd stage:

$$H_\xi(\boldsymbol{x},\boldsymbol{y})=\min_{\boldsymbol{u}}\sum_{w\in W}d^w\cdot\left(1-\sum_{j\in J}u_j^w(\xi)\right)\cdot l^w+\sum_{w\in W}\sum_{j\in J}u_j^w(\xi)\cdot\left(q_j^w+g_j\right),\ \forall\xi\in\Xi\quad(8)$$

subject to:

»» cargo flow assignment constraints:

» cargos are only transferred at a selected terminal, where the transfer flow is not more than the terminal capacity;

» cargos are only delivered on a determined land link subject to the opened connection, while the total flow on each land link used by the paths should not exceed its capacity;

» the total volume of cargo flow on each water link should not exceed its capacity:

$$\sum_{w\in W}d^w\cdot u_j^w(\xi)\le x_j\cdot c_j\cdot\left(1-\delta_j(\xi)\right),\ \forall j\in J,\ \forall\xi\in\Xi;\quad(9)$$

$$\sum_{k\in K} d^{w(i,k)} \cdot u_j^{w(i,k)}(\xi) \le y_{ij} \cdot a_{ij},$$
$$\forall i \in I,\ \forall j \in J,\ \forall \xi \in \Xi; \tag{10}$$
$$\sum_{i\in I} d^{w(i,k)} \cdot u_j^{w(i,k)}(\xi) \le a_{jk},$$
$$\forall j \in J,\ \forall k \in K,\ \forall \xi \in \Xi. \tag{11}$$

For constraint (Equation (11)), only the capacity limitations of some special water links will be taken into account.

»» freight demand constraints:

» for each disruption condition, there may be a portion of freight demands cannot be satisfied;

» for the normal condition, all the freight demands need to be satisfied:

$$\sum_{j\in J} u_j^w(\xi) \le 1,\ \forall w \in W,\ \{\xi \in \Xi \mid J_\xi \ne \phi\}; \tag{12}$$
$$\sum_{j\in J} u_j^w(\xi) = 1,\ \forall w \in W,\ \{\xi \in \Xi \mid J_\xi = \phi\}. \tag{13}$$

Constraint (13) requires that the capacity of opened paths can at least meet the total demands or preferably has some redundancy, otherwise when the initial setup of the network are too costly, the freight even in normal condition may take the price of loss from a portion of capacity shortage to guarantee the best total cost;

»» non-negative constraints:

$$u_j^w(\xi) \ge 0,\ \forall j \in J,\ \forall w \in W,\ \forall \xi \in \Xi. \tag{14}$$

In the 2nd stage model Equations (8)–(14), the unit loss is a penalty cost generally far greater than the unit freight cost. Thus the demand needs to be satisfied as far as possible for each scenario to reduce the recourse cost.

The risk-neutral model aims to strike a balance between the fixed cost and the expectation of variable costs. Under a given decision, the distribution of the variable cost is obtained, namely, the situation of freight reliability is figured out. Solutions of it are utilized to compare with those obtained with the MR model in the next subsection, in which risk appetites of decision-makers will be embedded.

2.3. Risk-averse decision-making

In worst-case, the impact of a potential disruption scenario could be unbearable. For instance, once several terminals on the heavily travelled paths are damaged simultaneously, the system will be unable to maintain even its basic function. The greater part of the normal transfer capacity is faced with critical degradation within the planning time zone. Therefore, the total cost for that scenario could reach to an extreme degree due to high losses from substantial amount of unsatisfied demands. Those high-impact events often arise with quite small probabilities, especially when the number of alternative terminals is relatively large.

The risk-averse decision-making adopts the mean-risk framework that combines CVaR with expectation to manage the volatility of costs, namely, the risk in financial meaning. CVaR focuses on costs that lie in the tail zone on the probability mass (Filippi *et al.* 2017). Although the worst-case costs can show great divergences from the expectation, the former, which are with low probabilities, may hardly contribute to the latter. For different cost mass functions, even if their expectations are figured out with similar values, the tail distributions are not always similar to or sometimes obviously distinct from each other, and vice versa. The optimality conditions for the EC and the tail costs are not mutually substitutable. Without loss of generality, for the path selection vectors $\boldsymbol{x}$ and $\boldsymbol{y}$, the CVaR of scenario costs $C_\xi = f_\xi(\boldsymbol{x}, \boldsymbol{y})$ under confidence level θ is defined as (Uryasev 2000):

$$CVaR_\theta(C_\xi) = (1-\theta)^{-1} \times \int_{VaR_\theta(C_\xi)}^{+\infty} f_\xi(\boldsymbol{x}, \boldsymbol{y}) \cdot \rho(\xi)\, d\xi, \tag{15}$$

where: $\rho(\xi)$ is the probability density of variable ξ representing the random factor that leads to uncertainties in cost; $VaR_\theta(C_\xi)$ is the VaR of C_ξ, and its definition is provided in:

$$VaR_\theta(C_\xi) = \inf\{\beta : \Pr(f_\xi(\boldsymbol{x}, \boldsymbol{y}) \le \beta) \ge \theta\}. \tag{16}$$

In Equation (16), $\Pr(\cdot)$ is the cumulative probability; if the random variable ξ follows a continuous distribution, then $VaR(C_\xi) = \beta$. As seen from the above 2 definitions, VaR is the θ-percentile on the distribution of total freight costs in an ascending order, which is the upper bound of the possible costs with the cumulative probability θ; while CVaR calculates the mean value of total freight costs of disruption scenarios that fall into the highest $(1-\theta)\cdot 100\%$ interval.

On the basis of the above analysis, now we develop our MR optimization with a bi-objective formulation, which is expressed in the weighted sum form: $E(C_\xi) + \lambda \cdot CVaR_\theta(C_\xi)$, where: $\lambda \in [0, +\infty)$ is the weight coefficient for risk aversion. Since disruptions are represented as scenario-specific, for the following modelling, we should firstly introduce the discrete transformation of CVaR as below (Rockafellar, Uryasev 2000):

$$CVaR_\theta(C_\xi) = \min_\alpha \alpha + (1-\theta)^{-1} \cdot \sum\nolimits_{\xi\in\Xi} P(\xi) \cdot \max(0, C_\xi - \alpha), \tag{17}$$

where: the CVaR is obtained by the above minimization problem and the solution of α is equal to the VaR. Rockafellar and Uryasev (2000) constructed an auxiliary relaxation $T(\xi)$ to linearize the term $\max[0, \cdot]$ in Equation (17), and the proposed MR model becomes:

MR:

$$\min E(C_\xi) + \lambda \cdot CVaR_\theta(C_\xi) =$$

$$\min_{\boldsymbol{x},\boldsymbol{y},\alpha}\sum_{j\in J}x_j\cdot h_j+\sum_{i\in I}\sum_{j\in J}y_{ij}\cdot t_{ij}+\sum_{\xi\in\Xi}P(\xi)\cdot H_\xi(\boldsymbol{x},\boldsymbol{y})+\lambda\cdot\left(\alpha+(1-\theta)^{-1}\cdot\sum_{\xi\in\Xi}P(\xi)\cdot T(\xi)\right) \quad (18)$$

subject to: constraints (Equations (3)–(7)), and:

»» risk constraints:

» differences between the costs of tail scenarios and the VaR are slacked:

$$\sum_{j\in J}x_j\cdot h_j+\sum_{i\in I}\sum_{j\in J}y_{ij}\cdot t_{ij}+\sum_{w\in W}d^w\cdot\left(1-\sum_{j\in J}u_j^w(\xi)\right)\cdot l^w+\sum_{w\in W}\sum_{j\in J}u_j^w(\xi)\cdot\left(q_j^w+g_j\right)-\alpha\le T(\xi),\ \forall\xi\in\Xi; \quad (19)$$

»» non-negativity constraints:

$$T(\xi)\ge 0,\ \forall\xi\in\Xi, \quad (20)$$

where: $H_\xi(\boldsymbol{x},\boldsymbol{y})$ is also defined by the 2nd stage model Equations (8)–(14); constraint (Equations (19) and (20)) separately forces the relaxations $T(\xi)$ no less than $C_\xi - \alpha$ for the tail scenarios and 0 for the other scenarios. The linearized risk term in the objective function is minimized by reducing relaxation variables $T(\xi)$ and calculating the VaR simultaneously.

Decision-makers now hold in hand both the parameters θ and λ to delimit the size of the subset of worst-case scenarios and to set the priority of risk control, respectively (Sawik 2011, 2013b). Assigning either of them the value 0 will degenerate the MR model into the risk-neutral form. As confidence level θ grows, the risk aversion follows with interest higher impact disruption scenarios, while the number of considered scenarios decreases. When $\lambda > 0$, the decision-maker starts trying risk controlling, and the risk preference becomes more intense with the greater weight. For a confidence level θ, the Pareto efficient frontier of the bi-objective programming can be obtained by solving the weighted sum model with the parameterization on λ. Unlike the risk-neutral model, which merely focuses on the average freight reliability, the risk-averse model will consider simultaneously improving the freight reliability in worst-case with further enhancement on capacity redundancy.

To facilitate solving the MR model with the decomposition algorithm introduced in the next section, we reformulate it as the following 2-stage MIP:

2-stage MR:

1st stage:

$$\min_{\boldsymbol{x},\boldsymbol{y},\alpha}\sum_{j\in J}x_j\cdot h_j+\sum_{i\in I}\sum_{j\in J}y_{ij}\cdot t_{ij}+\lambda\cdot\alpha+\sum_{\xi\in\Xi}P(\xi)\cdot Q_\xi(\boldsymbol{x},\boldsymbol{y},\alpha) \quad (21)$$

subject to: constraints (Equations (3)–(7)).

2nd stage:

$$Q_\xi(\boldsymbol{x},\boldsymbol{y},\alpha)=\min_{\boldsymbol{u},\boldsymbol{Z}}\sum_{w\in W}d^w\cdot\left(1-\sum_{j\in J}u_j^w(\xi)\right)\cdot l^w+\sum_{w\in W}\sum_{j\in J}u_j^w(\xi)\cdot\left(q_j^w+g_j\right)+\lambda\cdot(1-\theta)^{-1}\cdot T(\xi),\ \forall\xi\in\Xi \quad (22)$$

subject to: constraints (Equations (9)–(14)) and constraints (Equations (19) and (20)),

where the decision variables α and $T(\xi)$ are reassigned into the 1st stage and the 2nd stage, respectively. Similar to the 2-stage EC model, when the 1st stage decision is made, the 2nd stage problems in the 2-stage MR model for all scenarios are independent with each other. That structure of MIPs is known as the block-ladder (Freund 2004).

3. BD algorithm

The above proposed MIPs are faced with exponential explosion as the number of alternative terminals rises, e.g., for a transfer network with 10 origins and 10 destinations and 40 non-zero demand O–D pairs, when involving 8 alternative terminals, the number of variables and constraints are separately over 80000 and 200000, which will easily expand to be above 400000 and 500000 while there are 10 terminals, respectively. To solve MIPs, as NP-hard problems, there is no polynomial time algorithm so far. BD algorithm can be effective in breaking down the computational barriers when solving MIPs with a special block-ladder structure.

3.1. Variable partition and problem reformulation

BD is founded on duality theory (Benders 1962) as a special case of cutting-plane method. In this method, MIPs are decomposed into a *master problem* and smaller tractable *sub problems* by variable partitioning. The partition of variables is called BD. As for our study, the formulations of both the 2-stage EC model and 2-stage MR model already have master-subordinate layer structures. For simplicity, here firstly re-express the above 2-stage models in the matrix form:

Master problem:

$$F(\boldsymbol{s},\boldsymbol{u})=\min_{\boldsymbol{s}}(\boldsymbol{e}_1)^T\cdot\boldsymbol{s}+\sum_{\xi\in\Xi}P_\xi\cdot G_\xi(\boldsymbol{s}) \quad (23a)$$

subject to: $\boldsymbol{A}_1\cdot\boldsymbol{s}\le\boldsymbol{b}_1;\ \boldsymbol{s}\in\boldsymbol{S}$ (23b)

Sub problem:

$$G'_\xi(\boldsymbol{s})=G_\xi(\boldsymbol{s})-o_\xi=\min_{u}(\boldsymbol{e}_{2\xi})^T\cdot\boldsymbol{u}_\xi,\ \forall\xi\in\Xi \quad (24a)$$

subject to: $\boldsymbol{A}_{2\xi}\cdot\boldsymbol{u}_\xi\le\boldsymbol{b}_{2\xi}+\boldsymbol{E}_\xi\cdot\boldsymbol{s},\ J_\xi\ne\phi;$ (24b)

$\boldsymbol{A}^1_{2\xi}\cdot\boldsymbol{u}_\xi\le\boldsymbol{b}^1_{2\xi}+\boldsymbol{E}^1_\xi\cdot\boldsymbol{s},\ J_\xi=\phi$ for constraint (Equations (9)–(12)); (24c)

$$\boldsymbol{A}_{2\xi}^{2}\cdot\boldsymbol{u}_{\xi}=\boldsymbol{b}_{2\xi}^{2}+\boldsymbol{E}_{\xi}^{2}\cdot\boldsymbol{s},\ \ J_{\xi}=\phi\ \text{ for constraint (13);} \tag{24d}$$

$$\boldsymbol{u}_{\xi}\geq 0,\ \forall\xi\in\Xi. \tag{24e}$$

In the above expressions, all the 1st stage decision variables, including terminal and path selection decision $\boldsymbol{x}$, $\boldsymbol{y}$ and the VaR α (only for the MR model), are notated by the decision vector $\boldsymbol{s}$; $\boldsymbol{u}_{\xi}$ and P_{ξ} represent the flow assignment and the probability of scenario ξ; $G_{\xi}(\boldsymbol{s})$ substitutes the terms $H_{\xi}(\boldsymbol{x},\boldsymbol{y})$ and $Q_{\xi}(\boldsymbol{x},\boldsymbol{y},\alpha)$; $\boldsymbol{e}_1$ and $\boldsymbol{e}_{2\xi}$ are the coefficient vectors for the objective functions in the 2-stages; $\boldsymbol{A}_1$ and $\boldsymbol{S}$ denote the coefficient matrices for the constraints and domain of definition for decision variables in the 1st stage; $\boldsymbol{A}_{2\xi}$ and $\boldsymbol{E}$ (when $J_{\xi}=\phi$, $\left(\boldsymbol{A}_{2\xi}\right)^{T}=\left[\left(\boldsymbol{A}_{2\xi}^{1}\right)^{T},\left(\boldsymbol{A}_{2\xi}^{2}\right)^{T}\right]$ and $\left(\boldsymbol{E}_{\xi}\right)^{T}=\left[\left(\boldsymbol{E}_{\xi}^{1}\right)^{T},\left(\boldsymbol{E}_{\xi}^{2}\right)^{T}\right]$) represent the coefficient matrices for the constraints and variables in the 2nd stage; $\boldsymbol{b}_1$, o_{ξ} and $\boldsymbol{b}_{2\xi}$ (when $J_{\xi}=\phi$, $\left(\boldsymbol{b}_{2\xi}\right)^{T}=\left[\left(\boldsymbol{b}_{2\xi}^{1}\right)^{T},\left(\boldsymbol{b}_{2\xi}^{2}\right)^{T}\right]$ are constant terms.

It is clear that the sub problems (Equations (24)) are linear programming when the master problem variables are held fixed. The linear duals of the sub problems are constructed as:

$$\Phi_{\xi}(\boldsymbol{v})=\max_{\boldsymbol{v}}\left(\boldsymbol{v}_{\xi}\right)^{T}\cdot\left(\boldsymbol{b}_{2\xi}+\boldsymbol{E}_{\xi}\cdot\boldsymbol{s}\right),\ \forall\xi\in\Xi \tag{25a}$$

$$\text{subject to: } \left(\boldsymbol{A}_{2\xi}\right)^{T}\cdot\boldsymbol{v}_{\xi}\leq\boldsymbol{e}_{2\xi},\ \forall\xi\in\Xi; \tag{25b}$$

$$\boldsymbol{v}_{\xi}\leq 0,\ J_{\xi}\neq\phi; \tag{25c}$$

$$\boldsymbol{v}_{\xi}^{1}\leq 0,\ \ J_{\xi}=\phi\ \text{ for constraint (Equations (9)–(12));} \tag{25d}$$

$$\boldsymbol{v}_{\xi}^{2}\in\mathbb{R},\ \ J_{\xi}=\phi\ \text{ for constraint (Equation (13)),} \tag{25e}$$

where: $\boldsymbol{v}_{\xi}$ (when $J_{\xi}=\phi$, $\left(\boldsymbol{v}_{\xi}\right)^{T}=\left[\left(\boldsymbol{v}_{\xi}^{1}\right)^{T},\left(\boldsymbol{v}_{\xi}^{2}\right)^{T}\right]$) is the dual vector of $\boldsymbol{u}_{\xi}$. It can be seen that for $\forall\xi\in\Xi$ the feasible region of the dual problems (Equations (25)) is irrelevant to the master problem decision vector $\boldsymbol{s}$. Thus if any of the dual problem is proven to be infeasible, the corresponding original sub problem is unbounded or infeasible under arbitrary $\boldsymbol{s}$, thereafter, solving the 2-stage problem will result in unbounded or infeasible solutions. On the contrary, if all dual problems are feasible, when we apply an algorithm to solve them, exactly one of 2 cases will arise for each given dual problem: it has an optimal solution, or it is unbounded. As regard to dual problem ξ, let $\hat{\boldsymbol{V}}_{\xi}=\left\{\hat{\boldsymbol{v}}_{\xi}^{m}\middle|m\in M_{\xi}\right\}$ be the universal set of extreme points on the polyhedral angles of its feasible region and $\boldsymbol{\Gamma}_{\xi}=\left\{\boldsymbol{\gamma}_{\xi}^{n}\middle|n\in N_{\xi}\right\}$ be the universal set of its extreme rays. In the 1st case, the solution $\hat{\boldsymbol{v}}_{\xi}$ must be located at one of the extreme points, so the optimal objective value $\Phi_{\xi}(\hat{\boldsymbol{v}})=\left(\hat{\boldsymbol{v}}_{\xi}\right)^{T}\cdot\left(\boldsymbol{b}_{2\xi}+\boldsymbol{E}_{\xi}\cdot\boldsymbol{x}\right)=\max_{m\in M_{\xi}}\left(\hat{\boldsymbol{v}}_{\xi}^{m}\right)^{T}\cdot\left(\boldsymbol{b}_{2\xi}+\boldsymbol{E}_{\xi}\cdot\boldsymbol{x}\right)$, and the primitive problem can also reach its optimal value $G_{\xi}'(\hat{\boldsymbol{s}})=\Phi_{\xi}(\hat{\boldsymbol{v}})$; whereas in the 2nd case, the algorithm will return an extreme ray for the dual that satisfies $\left(\boldsymbol{\gamma}_{\xi}^{n}\right)^{T}\cdot\left(\boldsymbol{b}_{2\xi}+\boldsymbol{E}_{\xi}\cdot\boldsymbol{x}\right)>0$.

Benders' cuts can be listed by enumerating the extreme points/rays, and the 2-stage model is then rewrote as:

Full master problem:

$$F^{*}(\boldsymbol{s},\boldsymbol{z})=\min_{\boldsymbol{x},\boldsymbol{z}}\left(\boldsymbol{e}_1\right)^{T}\cdot\boldsymbol{s}+\sum_{\xi\in\Xi}P_{\xi}\cdot\left(\boldsymbol{z}_{\xi}+o_{\xi}\right) \tag{26a}$$

$$\text{subject to: } \left(\hat{\boldsymbol{v}}_{\xi}\right)\cdot\left(\boldsymbol{b}_{2\xi}+\boldsymbol{E}_{\xi}\cdot\boldsymbol{s}\right)\leq\boldsymbol{z}_{\xi},\ \forall\xi\in\Xi,\ \forall m\in M_{\xi}; \tag{26b}$$

$$\left(\boldsymbol{\gamma}_{\xi}^{n}\right)^{T}\cdot\left(\boldsymbol{b}_{2\xi}+\boldsymbol{E}_{\xi}\cdot\boldsymbol{s}\right)\leq 0,\ \forall\xi\in\Xi,\ \forall n\in N_{\xi}; \tag{26c}$$

$$\boldsymbol{A}_1\cdot\boldsymbol{s}\leq\boldsymbol{b}_1;\ \boldsymbol{s}\in\boldsymbol{S}. \tag{26d}$$

In Equation (26), the relaxation variables $\boldsymbol{z}_{\xi}$ and constraints (Equations (26b) and (26c)) replace the sub problems (Equations (24)). Herein $\boldsymbol{z}_{\xi}$ are also decision variables, which give the upper bounds to the objective values of the dual problems, namely, for $\forall\xi\in\Xi$, $\boldsymbol{z}_{\xi}\geq\max_{m\in M_{\xi}}\left(\hat{\boldsymbol{v}}_{\xi}^{m}\right)^{T}\cdot\left(\boldsymbol{b}_{2\xi}-\boldsymbol{E}\cdot\boldsymbol{x}\right)$. Any decision $\boldsymbol{x},\boldsymbol{z}_{\xi}$ that violates constraints (Equation (26b)) is identified as the non-optimal solutions for problem (Equations (26)) and can be eliminated. Constraints (Equation (26b)) are known as the Benders' optimality cuts. Unbounded duals of sub problems make the 2-stage problem infeasible, so decisions $\boldsymbol{x}$ that stand on extreme rays should be avoid with constraints (Equation (26c)), which are called the Bender feasibility cuts (Contreras *et al.* 2011; De Camargo *et al.* 2008; Marufuzzaman *et al.* 2014).

3.2. Solving procedures

In practice, BD usually begins with a restricted master problem that is constrained by just a subset of extreme points/rays and takes the price of iterations to gradually add subsets of Benders' cuts. Different solvers or algorithms can be employed to solve the master and the sub problems in the iteration process. The solving procedures are summarized below.

Solving procedures based on BD algorithm (see below).

Step 0. Define data sets. Determine the values of input parameters, then generate the probabilities and the capacities decline rates for scenarios. Select a confidence level θ and a risk coefficient λ.

Step 1. Initialize the problem. Let upper bound $UB=+\infty$ and lower bound $LB=-\infty$; set a gap ε; for all ξ, let both the extreme point set $\hat{\boldsymbol{V}}_{\xi}$ and the extreme ray set $\boldsymbol{\Gamma}_{\xi}$ be $\varnothing$.

Step 2. Solve the master problem (Equations (26)) with Benders' cuts corresponding to $\hat{\boldsymbol{V}}_{\xi}$ and $\boldsymbol{\Gamma}_{\xi}$.

»» if the master problem is infeasible, then break;

»» if the solution is $\overline{\boldsymbol{s}},\overline{\boldsymbol{z}}_{\xi}$ and the objective value $F^{*}(\overline{\boldsymbol{s}},\overline{\boldsymbol{z}}_{\xi})\geq LB$, then update the lower bound as $LB=F^{*}(\overline{\boldsymbol{s}},\overline{\boldsymbol{z}}_{\xi})$; turn to ***Step 3***.

Step 3. Solve the dual sub-problems (Equations (25)) for all ξ with $\boldsymbol{s}=\overline{\boldsymbol{s}}$ and generate Benders' cuts:

»» if any dual sub-problem ξ is infeasible, then break; problem (23) is infeasible or unbounded;

»» if each dual sub-problem returns an optimal solution, then get solutions $\hat{\boldsymbol{v}}_\xi$ for dual sub-problems (Equations (25)) and $\overline{\boldsymbol{u}}_\xi$ for primary sub-problems (Equations (24)), and 2 cases will rise below:

» for $\forall\xi$, if $\hat{\boldsymbol{v}}_\xi$ satisfies $\left(\hat{\boldsymbol{v}}_\xi\right)^T\cdot\left(\boldsymbol{b}_{2\xi}+\boldsymbol{E}_\xi\cdot\overline{\boldsymbol{s}}\right)\le\overline{z}_\xi$, then break; return $F\left(\overline{\boldsymbol{s}},\overline{\boldsymbol{u}}_\xi\right)$ as the optimal objective value and $\overline{\boldsymbol{s}},\overline{\boldsymbol{u}}_\xi$ as the solution;

» for some ξ, if $\hat{\boldsymbol{v}}_\xi$ satisfies $\left(\hat{\boldsymbol{v}}_\xi\right)^T\cdot\left(\boldsymbol{b}_{2\xi}+\boldsymbol{E}_\xi\cdot\overline{\boldsymbol{s}}\right)>\overline{z}_\xi$, then add $\hat{\boldsymbol{v}}_\xi$ into the set $\hat{\boldsymbol{V}}_\xi$, and if $F\left(\overline{\boldsymbol{s}},\overline{\boldsymbol{u}}_\xi\right)\le UB$, then update $UB=F\left(\overline{\boldsymbol{s}},\overline{\boldsymbol{u}}_\xi\right)$; go to ***Step 4***;

»» otherwise, get the solutions $\hat{\boldsymbol{v}}_\xi$ for some ξ and the extreme rays $\boldsymbol{\gamma}_\xi$ for the others in dual sub-problems (Equations (25)), then add extreme points $\hat{\boldsymbol{v}}_\xi$ that satisfy $\left(\hat{\boldsymbol{v}}_\xi\right)^T\cdot\left(\boldsymbol{b}_{2\xi}+\boldsymbol{E}_\xi\cdot\overline{\boldsymbol{s}}\right)>\overline{z}_\xi$ (if any) into the set $\hat{\boldsymbol{V}}_\xi$ and add extreme rays $\boldsymbol{\gamma}_\xi$ into the set $\boldsymbol{\Gamma}_\xi$; return to ***Step 2***.

Step 4. Check bounds:

»» if $\dfrac{UB-LB}{UB}\le\varepsilon$, then break and take UB as the optimal objective value and $\overline{\boldsymbol{s}},\overline{\boldsymbol{u}}_\xi$ as the solution;

»» otherwise, return to ***Step 2***.

4. Computational examples

Several numerical cases are presented in this section to justify the feasibility of the proposed models. The confidence level and the risk term weight are set at different grades to illustrate how the risk preferences of the decision-maker influence the selection of paths and terminals. All the computational experiments are programmed in *CPLEX Optimization Studio V12.8* (*https://www.ibm.com/support/pages/cplex-optimization-studio-v128*) under *Microsoft Windows 10* environment, running on a laptop with *Intel Core i5-6200u* processor and 8GB RAM.

4.1. Input datasets

We consider a port cluster with 10 terminals serves 10 demand areas in its landward hinterland. Cargos are imported from/exported to 10 oversea ports. For instance, there is a series of ports located in the coastal region of Bohai bay in north China, like Tianjin, Qingdao, Qinhuangdao, Tangshan, Yantai, Rizhao, Weihai, Huanghua and so on, each of which has one or several independent port areas that can be separately used as transfer terminals. Those ports are geographically close to each other, and the landward hinterlands of them are largely overlapped. They normally serve intermodal freight related to many hinterland cities in Hebei, Shandong, Shanxi, Henan, Shaanxi and other provinces. Cargos mainly including coal, steel, ore, oil and containers travel by rail or road between the ports and the landward hinterlands and are carried with vessels to/from endpoint ports at the seaward side like South Korea, Japan, Australia, South America and South China. This HPFN is in harmony with the structure depicted in Figure 1.

The input parameters are based on random data. Let the capacities of terminals c_j [10^4 ton] be integers randomly exacted with equal probabilities from set {50, 60, 70, 80, 90, 100, 110, 120, 130, 140, 150}, generated from a $10\cdot\mathrm{int}\left(U\left(5,15\right)\right)$ distribution; similarly, the capacities of land links a_{ij} [10^4 ton] are drawn from a uniform distribution $0.5\cdot\mathrm{int}\left(U\left(6,36\right)\right)$; the number of non-zero demand O–D pairs is set as 40 and the demands of them are generated from an uniform distribution $0.2\cdot\mathrm{int}\left(U\left(20,50\right)\right)$; suppose the vessels can be easily dispatched in the port cluster region, so the water link capacities in our cases are without boundaries.

Fixed costs t_{ij} [$\$10^4$] of setting up connecting agencies are integers in set {6, 7, 8, 9, 10, 11, 12, 13, 14, 15, 16}, exacted from a uniform distribution $\mathrm{int}\left(U\left(6,16\right)\right)$; fixed costs h_j [$\$10^4$] for setting storage places are integers drawn from a uniform distribution $5\cdot\mathrm{int}\left(U\left(30,60\right)\right)$; the budget for total fixed cost B [$\$10^4$] is equal to 3000.

The unit variable cost for a path used by an O–D pair is constituted of the unit cost of transportation on the land and water link and the unit cost of transhipping at the terminal. The former varies with the lengths of both of the links, determined by the topological structure of networks. The costs for a unit of cargo transportation q_j^w [$/ton] are also drawn all at once from a uniform distribution $0.2\cdot\mathrm{int}\left(U\left(20,50\right)\right)$. Besides, the unit transhipping costs g_j [$/ton] are produced with a uniform distribution $0.5\cdot\mathrm{int}\left(U\left(4,8\right)\right)$. For all the 40 O–D pairs, the values of unit losses from unsatisfied demand l^w [$/ton] are given as 500.

The probability of disastrous events in the port cluster region is set as τ = 0.8. Probabilities for the terminals disrupted in the events is given as {0.08, 0.1, 0.1, 0.12, 0.14, 0.16, 0.18, 0.20, 0.20, 0.22}, in which p_j increase with the growth of j. The rates of capacity declines δ_j for the terminals, by contrast, is in a descending order as j grows, defined as {0.85, 0.80, 0.75, 0.75, 0.70, 0.70, 0.65, 0.65, 0.60, 0.55}. Those settings of probabilities and decline rates can be real if the planning is for some special periods, like the hurricane or flood season. There are 1024 disruption scenarios, and the probability of the normal scenario without capacity decline at any terminal is 0.355, which is quite a large value relative to the probabilities of disruption scenarios, e.g., the probability of the scenario where only terminal j = 4 affected is 0.021; when all terminals are affected, the scenario probability is down to $2.7\cdot10^{-9}$.

4.2. Simulation results

According to the above rules, the data sampling is implemented in MATLAB (*https://www.mathworks.com/products/matlab.html*) to obtain all the input parameters, where the total transportation demand of O–D pairs is

$\sum_{w\in W} d_w = 269.8$, and the total capacity of land links and terminals are $\sum_{i\in I}\sum_{j\in J} a_{ij} = 1120$ and $\sum_{j\in J} c_j = 1050$, respectively. For the illustration examples, let the number of alternative terminals be 10 and 8. The 10-terminal example takes all the 10 terminals in the port cluster for selection, labelled by 10–1. The 8-terminal example considers 2 cases separately labelled by 8–1 and 8–2, and the former uses terminals j = 1, 2, …, 8 while the latter uses terminals j = 3, 4, …, 10 as alternatives. Comparing with case 8–1, alternative terminals in case 8–2 are faced with higher disruption probabilities but lighter consequences. Confidence level θ is set at 4 grade as {0.75, 0.90, 0.95, 0.99}. Let weight coefficient of the risk term λ ∈{0, 0.05, 0.25, 0.50, 1.00, 10.00}.

Optimization outcomes shown in Tables 3–6 for the 3 cases are figured out by applying the BD algorithm with termination gap ε = 0.01%. Tables 3–6 also present the running durations to prove the optimality of the solutions. All the test examples can be solved within CPU seconds. Comparing the outcomes between the 2 case with 8 alternative terminals and case 10–1, it is found that, with application of the 2-stage EC model, the optimal total EC of the former 2 cases is greater than that of the last one, and when applying the 2-stage MR model, the same happens for both the optimal expectation and the CVaR of the overall cost. Deciding a broader set of alternative terminals for selection seems to be better for reducing the total cost in practice.

Both confidence level θ and weight coefficient λ reflect the risk appetites of decision-makers. Figure 3 draws how the terminal and connection/land link selection costs change with the 2 parameters, where the outcomes for θ = 0 is from the 2-stage EC model as shown in Table 3. It indicates that, when we raise the 2 parameters, the total fixed cost takes on upward trends in general, which results in more redundant strategies of network capacity design. Therefore, once network planners start to consider risk aversion to mitigate the impact of tail disruption scenarios, they should prepare higher fixed input budgets for opening and maintaining intermodal paths at the very beginning of the planning period, and more aggressive risk aversions will lead to more expensive network resource allocation decisions.

In particular, it can be seen in Figure 3, with the increase of θ in case 10–1, the terminal selection cost expands stably, however, once the terminal selection cost jumps, the growth of connection selection cost is reversed, which returns to growth after the reversion. That rule is also found in any other of the outcome data sets. That implies, regardless of the priority of risk control, if the decision-maker tries to mitigate higher impact scenarios, enough terminal capacities should be guaranteed firstly and then more link capacities subject to the opening of connections can be selected to make use of the terminal capacities as full as possible.

We are interested in the dynamics of the expectation and the CVaR of total cost that follow the change of the risk weight in the bi-objective model. The outcomes exhibited in Tables 3–6 reveal that, under the same confidence level, the total EC increases with weight λ, while the CVaR, which is the mean total cost of the worst-case scenarios, decreases as λ is enlarged. For instance, in case 8–1, the minimized expectation/CVaR separately rises/falls from 668.207/1040.392 (λ = 0) to 692.628/707.934 (λ = 10) for confidence level θ = 0.99, and for θ = 0.75, those values change from 668.207/685.395 (λ = 0) to 674.179/681.362 (λ = 10). The minimizations of the 2 objectives are a trade-off, which can be emphasized with the Pareto frontier curved in Figure 4. Therefore, although the higher priority of risk control means the better cost reductions of the worst-case scenarios defined by a given confidence level, it is wise for the decision-maker to decide the risk weight cautiously in order to avoid excessive EC values in some cases.

Figures 5–7 plot the breakdown of the optimal objective value of case 10–1, which facilitate understanding the differences of the costs between confidence levels. A greater θ accounts for a greater CVaR of total costs in Figure 5 at each grade of the risk weights. That is to be expected because a lager confidence level determines a higher percentile from which the worst-case zone starts. Figure 6 indicates that the expectation of total cost increases as θ increases under each λ. Moreover, for a larger θ, the rate that the optimal CVaR/expectation of total cost decreases/increases as λ increases will be grater, i.e., for θ = 0.75, 0.90, 0.95, 0.99, when λ is raised from 0 to 10 in case 10–1, the CVaR will grade down by 0.92, 3.86, 8.74, 34.96%, while the expectations increase by 0.98, 1.29, 1.29, 3.52%, respectively. It provides decision-makers an insight that, when they try to hedge against the cost of scenarios in a higher tail zone, it is worth weighting the risk term greater, which brings about a more thorough reduction of the tail mean total cost but with merely a subtle increase in total EC for those specific cases.

As shown in Figure 7, the total fixed cost also increases with θ. The shape of the surface drawing in Figure 7 is quite similar to that in Figure 6, and the rates of the fixed cost in the total cost are at around 25% in general. As the risk parameters grow, the expected variable cost, which is the difference between the total EC and the fixed cost, is not reduced in proportion with the increase of the fixed cost, e.g., according to the outcomes in Table 3 and Table 6, when λ = 1, θ = 0.99, the expected variable cost is 490.812, which is 16.181 (= 506.993 – 490.812) or 3.19% lower than the 2-stage EC model, however, the fixed costs are separately 148.9 for the 2-stage EC and 187.2 for the 2-stage MR, showing a increment of 38.3 or 25.72%. The expected variable cost indicates the freight reliability from an average-performance perspective. That implies, applying the risk-averse model, which seeks a further enhancement on capacity redundancy with more fixed cost, may be not a cost-effective way to improve the average freight reliability. In other words, with the application of the risk-neutral model, the average freight reliability already achieves a desirable level.

Table 3. Solutions of 2-stage EC model (cost [$\$10^5$])

Alternative terminals		θ				EC	No of selected terminals (fixed cost)	No of opened connections (fixed cost)	Time [s]
		0.75	0.90	0.95	0.99				
8–1	CVaR	685.395	710.363	749.497	1040.392	668.207	5 (106.0)	41 (43.8)	49
	VaR	668.100	669.810	673.350	680.500				
8–2	CVaR	681.861	713.066	762.283	1142.492	663.818	5 (110.5)	37 (37.6)	47
	VaR	660.620	662.970	664.700	675.620				
10–1	CVaR	674.071	700.526	743.706	1061.030	655.893	5 (112.0)	36 (36.9)	503
	VaR	654.510	656.440	661.520	674.230				

Table 4. Solutions of 2-stage MR model for case 8–1 (cost [$\$10^5$])

λ	0.05				0.25				0.50	
θ	0.75	0.90	0.95	0.99	0.75	0.90	0.95	0.99	0.75	0.90
CVaR	685.395	710.363	737.729	783.720	683.636	704.738	702.016	749.382	683.636	692.841
VaR	668.100	669.810	674.330	685.340	669.200	670.040	680.150	686.730	669.200	676.670
EC	668.207	668.207	668.592	674.540	668.592	668.592	674.540	677.558	668.592	673.220
No of selected terminals (fixed cost)	5 (106)	5 (106)	5 (106)	6 (121)	5 (106)	5 (106)	6 (121)	6 (121)	5 (106)	6 (121)
No of opened connections (fixed cost)	41 (43.8)	41 (43.8)	42 (44.9)	42 (42.7)	42 (44.9)	42 (44.9)	42 (42.7)	46 (47.4)	42 (44.9)	41 (42.1)
Time [s]	69	60	94	35	59	72	63	53	79	73

λ	0.5		1.0				10.0			
θ	0.95	0.99	0.75	0.90	0.95	0.99	0.75	0.90	0.95	0.99
CVaR	698.956	709.270	683.636	689.905	698.956	707.934	681.362	689.378	697.257	707.934
VaR	681.100	699.510	669.200	678.190	681.100	700.810	673.890	678.990	683.200	700.810
EC	675.649	691.466	668.592	674.982	675.649	692.628	674.179	675.649	677.558	692.628
No of selected terminals (fixed cost)	6 (121.0)	7 (147.5)	5 (106.0)	6 (121.0)	6 (121.0)	7 (147.5)	6 (121.0)	6 (121.0)	6 (121..0)	7 (147.5)
No of opened connections (fixed cost)	44 (45.3)	42 (41.8)	42 (44.9)	43 (44.5)	44 (45.3)	43 (42.0)	42 (43.6)	44 (45.3)	46 (47.4)	43 (42.0)
Time [s]	49	206	51	49	42	101	73	55	58	252

Table 5. Solutions of 2-stage MR model for case 8–2 (cost [$\$10^5$])

λ	0.05				0.25				0.50	
θ	0.75	0.90	0.95	0.99	0.75	0.90	0.95	0.99	0.75	0.90
CVaR	681.861	713.066	744.587	738.162	680.679	704.854	689.955	715.884	679.492	692.160
VaR	660.620	662.970	666.100	681.150	661.340	664.550	676.760	683.790	662.150	669.620
EC	663.818	663.818	664.398	673.384	664.094	664.398	673.384	675.731	664.398	668.167
No of selected terminals (fixed cost)	5 (110.5)	5 (110.5)	5 (110.5)	6 (132.5)	5 (110.5)	5 (110.5)	6 (132.5)	6 (132.5)	5 (110.5)	5 (117.5)
No of opened connections (fixed cost)	37 (37.6)	37 (37.6)	39 (39.3)	35 (33.6)	38 (38.5)	39 (39.3)	35 (33.6)	37 (36.1)	39 (39.3)	37 (38.0)
Time [s]	30	34	32	103	28	66	168	67	30	116

λ	0.50		1.00				10.00			
θ	0.95	0.99	0.75	0.9	0.95	0.99	0.75	0.9	0.95	0.99
CVaR	687.534	702.393	679.492	682.860	687.534	699.089	677.922	682.198	686.871	698.295
VaR	677.830	690.900	662.150	675.300	677.830	693.300	667.900	676.400	678.830	694.410
EC	674.307	681.548	664.398	673.384	674.307	683.818	668.539	674.307	676.271	684.899
No of selected terminals (fixed cost)	6 (132.5)	6 (141.0)	5 (110.5)	6 (132.5)	6 (132.5)	6 (141.0)	5 (117.5)	6 (132.5)	6 (132.5)	6 (141.0)
No of opened connections (fixed cost)	36 (34.7)	33 (34.0)	39 (39.3)	35 (33.6)	36 (34.7)	35 (36.4)	37 (38.4)	36 (34.7)	37 (36.7)	36 (37.5)
Time [s]	131s	66s	37s	196s	88s	77s	135s	130s	53s	90s

Table 6. Solutions of 2-stage MR model for case 10–1 (cost [10^5])

λ	0.05				0.25				0.50	
θ	0.75	0.90	0.95	0.99	0.75	0.90	0.95	0.99	0.75	0.90
CVaR	670.316	691.872	723.977	734.163	670.316	688.303	681.915	710.942	670.316	673.983
VaR	655.220	657.300	662.450	671.360	655.220	657.610	666.860	673.380	655.220	665.680
EC	655.924	655.924	655.924	662.390	655.924	656.568	662.390	664.218	655.924	662.390
No of selected terminals (fixed cost)	5 (112)	5 (112)	5 (112)	6 (127)	5 (112)	5 (112)	6 (127)	6 (127)	5 (112)	6 (127)
No of opened connections (fixed cost)	37 (38.1)	37 (38.1)	37 (38.1)	38 (37.1)	37 (38.1)	38 (39.3)	38 (37.1)	40 (39.4)	37 (38.1)	38 (37.1)
Time [s]	1041	1025	1206	1027	899	822	837	1016	661	1947

λ	0.5		1.0				10.0			
θ	0.95	0.99	0.75	0.90	0.95	0.99	0.75	0.90	0.95	0.99
CVaR	680.335	707.972	669.442	673.983	678.725	690.631	667.872	673.461	678.725	690.047
VaR	668.380	674.390	656.420	665.680	668.920	685.600	662.780	668.060	668.920	684.530
EC	663.131	665.168	656.568	662.390	664.323	678.021	662.390	664.323	664.323	678.949
No of selected terminals (fixed cost)	6 (127.0)	6 (127.0)	5 (112.0)	6 (127.0)	6 (127.0)	7 (150.5)	6 (127.0)	6 (127.0)	6 (127.0)	7 (149.0)
No of opened connections (fixed cost)	39 (38.3)	41 (40.4)	38 (39.3)	38 (37.1)	40 (39.6)	36 (36.7)	38 (37.1)	40 (39.6)	40 (39.6)	35 (35.0)
Time [s]	968	859	2197	1114	1182	6477	1316	835	918	3213

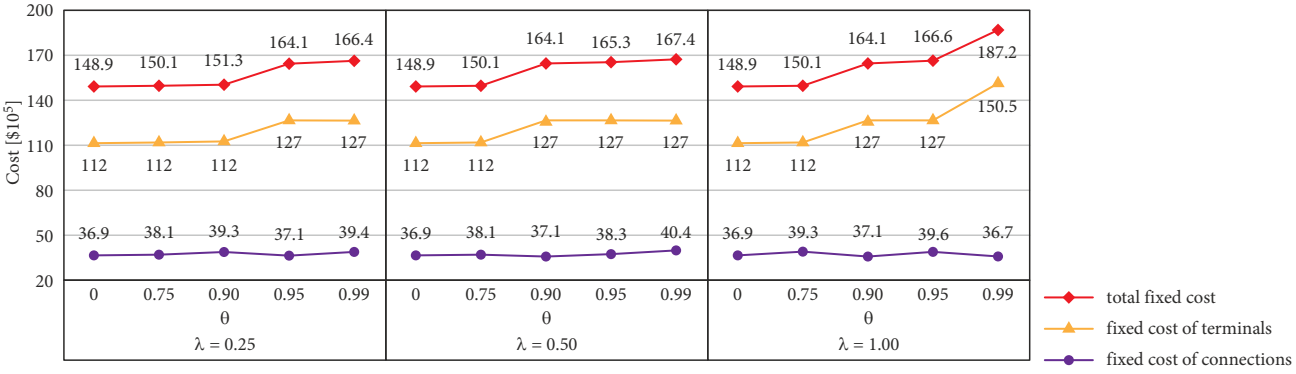

Figure 3. Terminal and connection selection costs for case 10–1

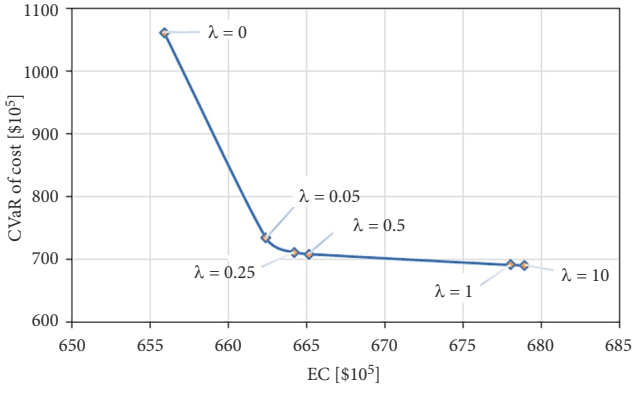

Figure 4. The Pareto frontier for case 10–1 with θ = 0.99

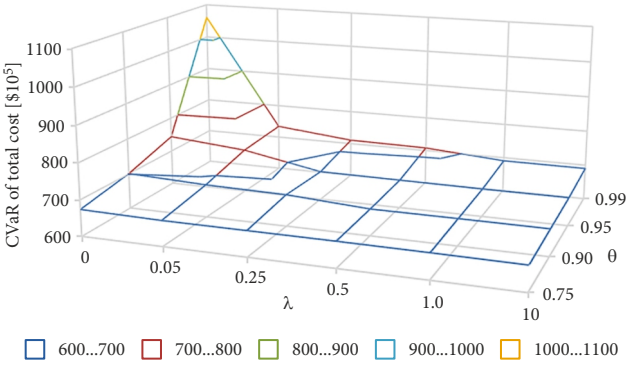

Figure 5. The optimal CVaR under different confidence levels for case 10–1

With regard to the variable costs of scenarios, although their expectation changes subtly, differences between the probability distributions of them are clearly observed under different risk parameters. The mass function of the variable costs for case 10–1 by applying the 2-stage EC model and the 2-stage MR model (also with $\lambda = 1$, $\theta = 0.99$) are separately displayed in Figures 8 and 9. The largest value of scenario costs is around 5450 for the risk-neutral model, while for the risk-averse model, it decreases roughly to 2550, that is, the tail variable costs are drastically reduced, meaning the strategies of network design and flow assignment generated from the risk-averse model can substantially guarantee the freight reliability in worst-cases.

In addition, the probability that the freight is operated without any loss is the indicator of absolute freight reliability. In Figures 8 and 9, those probabilities are associated with the lowest points on the distribution of variable costs of scenarios. Both of them are close to 0.6, larger

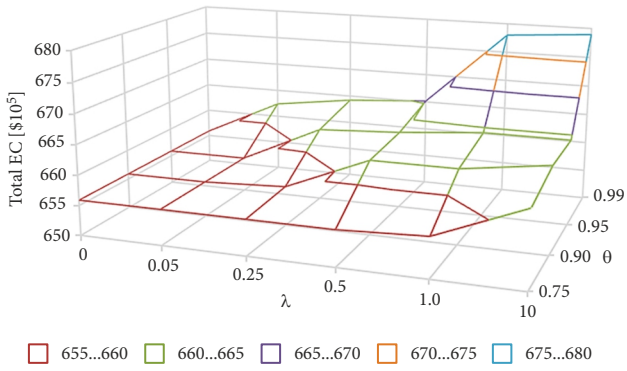

Figure 6. The optimal EC under different confidence levels for case 10–1

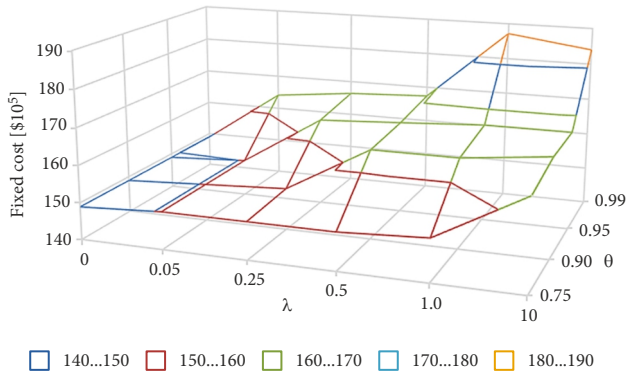

Figure 7. The optimal fixed cost under different confidence levels for case 10–1

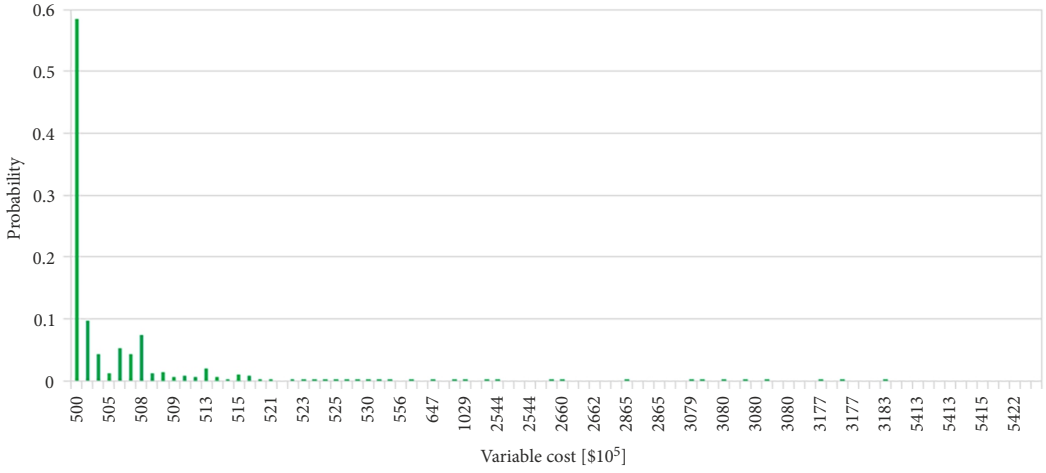

Figure 8. The probability mass function of variable costs of scenarios for case 10–1: $\lambda = 0$

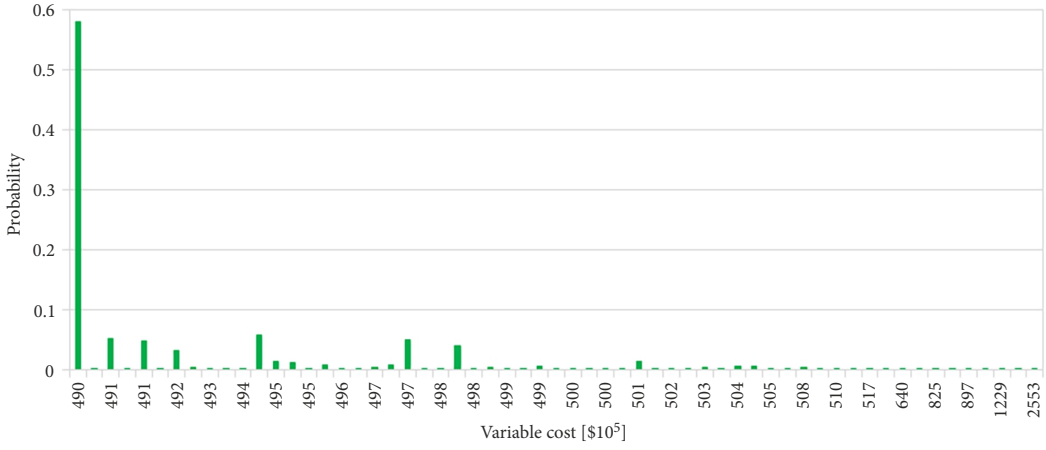

Figure 9. The probability mass function of variable costs of scenarios for case 10–1: $\lambda = 1$, $\theta = 0.99$

than the probability of the normal condition without capacity decline at any terminal in the port cluster, which is equal to 0.355. In this sense, adopting both the models can effectively protect the intermodal process from disruption events.

4.3. Algorithm performance

The efficiency and accuracy of BD algorithm for the proposed examples is justified by comparing it with the *CPLEX Optimization Studio V12.8* solver and the BBD. BBD shares the same theoretical basis and running procedures with BD. However, BBD makes all the continuous variables into a single sub-problem (Freund, 2004), ignoring the block-ladder structure of the 2-stage stochastic model, and the aggregation of the objectives for all scenarios in the 2nd stage problems is used as the objective function of the sub-problem.

Table 7 gives the compute results by using different algorithms with the termination gap 0.01%. The solving time grows rapidly as the number of alternative terminals increases from 8 to 10 for all cases, because the number of variables, constraints and non-zero coefficients all increase by several times. In case 10–1, when using the *CPLEX Optimization Studio V12.8* solver, the relative gaps are still over 5% after 5 h of the time limit, while the 2 Benders' algorithms can solve all the test cases in CPU seconds and both run fast than the *CPLEX Optimization Studio V12.8* solver. Since BBD generates one cut (feasibility cut or optimality cut) at each iteration step, it is much less efficient in obtaining active constraints than BD hence generally converges slower (see column 7 and column 10 of Table 7). Furthermore, each solved case by applying different algorithms converge at the same objective value. Notice that the 10–1 case have more than 400000 variables and more than 550000 constraints, and it is still manageable with the 2-stage stochastic formulation and the BD algorithm to solve. However, for a 15-terminal problem with the same number of O–D pairs, the number of both variables and constraints can be more than 20000000. In this case, the proposed decomposition algorithm will not help much because it is intractable for even the construction of the problem in the computing environment (Sawik 2013b; Noyan 2012).

Conclusions

The main contribution of this work is the formulation of scenario-based 2-stage stochastic MIPs for the reliable planning of the HPFN from the perspective of port users at the system level. This paper introduced the concept of reliability to hinterland-port freights, which is defined as the level of freight demand satisfaction. Due to the dominance of the loss in the variable cost, the freight reliability can be depicted by the variable cost comprising the cost of cargo travel and the loss from unsatisfied demands, and the larger the variable cost, the lower the reliability. The proposed models allow HPFN planners to decide network capacities ahead of time with precise estimation of probability distribution of variable costs, hence to figure out the desirable freight reliability by balancing the fixed cost and possible variable costs. The selection of network capacities, which include redundancy preparedness, can be figured out in both a risk-neutral and a risk-averse environment. The risk-averse model, which combines the CVaR criterion with the expectation criterion, shows HPFN planners a simple approach to quantify their risk appetites and to impose them in the decision process for trading off the 2 criteria. As such, HPFN planners are able to know the minimal uncertainty of costs in the face of disruptions of in the form of exact worst-case cost.

The optimality of the limited test cases based on random datasets were all proven by performing BD algorithm, which takes advantage of the block-ladder structure of the optimization models for solving without undue memory and time consumptions. Some valuable insights were observed from the simulation results: 1st, including more terminals in the alternative set may result in lower

Table 7. Performance comparisons between algorithms

Cases	Models	*CPLEX* solver			BBD			BD		
		Objective value [$\cdot 10^5$]	Time [s]	Gap [%]	Objective value [$\cdot 10^5$]	Time [s]	Gap [%]	Objective value [$\cdot 10^5$]	Time [s]	Gap [%]
8–1	2-stage EC[a]	668.207	1534	0.03	668.207	99	0.09	668.207	49	0.10
	2-stage MR[b]	1374.605	974	1.42	1374.605	145	0.09	1374.605	42	0.08
8–2	2-stage EC[a]	663.818	1198	0.01	663.818	54	0.03	663.818	47	0.04
	2-stage MR[b]	1361.842	1303	0.08	1361.842	251	0.02	1361.842	88	0.02
10–1	2-stage EC[c]	–	–	–	655.893	1374	0.02	655.893	503	0.03
	2-stage MR[d]	–	–	–	1343.048	5440	0.03	1343.048	1182	0.02

Notes:

[a] – No of binary variables N_{bv} = 88, No of continuous variables N_{cv} = 81920, No of constraints N_{con} = 114716, No of non-zero coeficients N_{nz} = 350560;

[b] – N_{bv} = 88, N_{cv} = 82177, N_{con} = 114972, N_{nz} = 455520, $\lambda = 1$, $\theta = 0.95$;

[c] – N_{bv} = 110, N_{cv} = 409600, N_{con} = 563232, N_{nz} = 1751480;

[d] – N_{bv} = 110, N_{cv} = 410625, N_{con} = 564256, N_{nz} = 2275768, $\lambda = 10$, $\theta = 0.95$.

values of both the EC and the tail mean cost; 2nd, as the risk parameters turns lager, the tail mean total cost can be discernibly reduced with slight increase of the total EC that is mainly attributed to the growth of fixed cost especially for terminal selection; 3rd, when the target scenarios are located in a higher tail zone, it is worthy of adopting a greater risk weight to more thoroughly control the worst-case cost; at last, comparing with the risk-neutral model, the risk-averse model may not lead to a significant further improvement of the average freight reliability, while it can substantially enhance the freight reliability in worst-cases, and both the models can guarantee desirable absolute freight reliability.

In practice, the flow assignment is always not an one-off but a continuous process of adjustment to uncertainties in demands generating and disruptions emerging over time. Precise planning should be based on full and detailed prediction of those dynamics, which, however, can be hardly achieved. Considering a multi-period optimization is able to narrow the gap between the static optimization and the empirical decisions. An as reasonable as possible segment of the planning period allows decision-makers to decide from when and how much value to allocate the capacities and assign the flows so as to boost the accuracy of outcomes.

The scope of port disruptions is confined in region-wide. That simplicity shall be slacked for the whole door-to-door freight network vulnerable to some super events impacting terminals on both sides of the water links simultaneously, including widespread labour strike, bankruptcy caused by global economic crisis and mega earthquake or hurricane, etc. It is necessary to integrate both the local and global events with reconstruction of disruption scenarios (Sawik 2011). The basic thoughts are similar to the proposed models except some additional constraints for the flow equilibrium at terminals.

Several relatively small problem instances were studied. However, the further growth of the exponential many disruption scenarios still increases the magnitude of variables and constraints hence jumps up the duration of solving, which handicaps the model application. To represent large size real-word problems or to extend the model into multi-period or complete topology settings (both raise the problem scale) for better fidelity, 2 immediate enhancements from computational view in the future work can be explored: 1st, finding stable methods for the reduction of disruption scenarios; 2nd, developing heuristic algorithms to seek out the global approximate solution instead of the precise solution but in higher computing speeds. Since the number of disruption scenarios also grows with terminal damage levels, decision-makers should pay attention to determining proper damage states for terminals, hence to balance the efficiency and the accuracy of the decision-making.

The estimation of disruption probabilities and resulting impacts directly determines the quality of decision, so it shall be implemented in a rigorous environment when studying empirical cases. Meanwhile, the site-dependent setting of the probabilistic disruptions shall be adopted with highly detailed delimiting of transfer nodes to avoid the correlations among sites (e.g., Shen *et al.* 2011; Li, Ouyang 2010).

Funding

This research is supported by the National Natural Science Foundation of China (Grant No 51379171) and the Fundamental Research Funds for the Central Universities (WUT: 2022IVA008).

Contribution

Each author has participated and contributed sufficiently to take public responsibility for appropriate portions of the content.

Disclosure statement

No potential conflict of interest was reported by the authors.

References

Benders, J. F. 1962. Partitioning procedures for solving mixed-variables programming problems, *Numerische Mathematik* 4(1): 238–252. https://doi.org/10.1007/bf01386316

Blake, E. S.; Zelinsky, D. A. 2017. *Tropical Cyclone Report: Hurricane Harvey* (*AL092017*). National Hurricane Center, Miami, FL, US. 77 p. Available from Internet: https://www.nhc.noaa.gov/data/tcr/AL092017_Harvey.pdf

Brunet, S.; De la Llera, J. C.; Jacobsen, A.; Miranda, E.; Meza, C. 2012. Performance of port facilities in Southern Chile during the 27 February 2010 Maule earthquake, *Earthquake Spectra* 28(S1): S553–S579. https://doi.org/10.1193/1.4000022

Carturan, F.; Pellegrino, C.; Rossi, R.; Gastaldi, M.; Modena, C. 2013. An integrated procedure for management of bridge networks in seismic areas, *Bulletin of Earthquake Engineering* 11(2): 543–559. https://doi.org/10.1007/s10518-012-9391-6

Chen, H.; Cullinane, K.; Liu, N. 2017. Developing a model for measuring the resilience of a port-hinterland container transportation network, *Transportation Research Part E: Logistics and Transportation Review* 97: 282–301. https://doi.org/10.1016/j.tre.2016.10.008

Chen, H.-H.; Yang, C.-B. 2017. Multiperiod portfolio investment using stochastic programming with conditional value at risk, *Computers & Operations Research* 81: 305–321. https://doi.org/10.1016/j.cor.2016.11.011

Chen, L.; Miller-Hooks, E. 2012. Resilience: an indicator of recovery capability in intermodal freight transport, *Transportation Science* 46(1): 109–123. https://doi.org/10.1287/trsc.1110.0376

Contreras, I.; Cordeau, J.-F.; Laporte, G. 2011. Benders decomposition for large-scale uncapacitated hub location, *Operations Research* 59(6): 1477–1490. https://doi.org/10.1287/opre.1110.0965

Cordeau, J.-F.; Stojković, G.; Soumis, F.; Desrosiers, J. 2001. Benders decomposition for simultaneous aircraft routing and crew scheduling, *Transportation Science* 35(4): 375–388. https://doi.org/10.1287/trsc.35.4.375.10432

Cui, T.; Ouyang, Y.; Shen, Z.-J. M. 2010. Reliable facility location design under the risk of disruptions, *Operations Research* 58(4): 998–1011. https://doi.org/10.1287/opre.1090.0801

De Camargo, R. S.; Miranda, G.; Luna, H. P. 2008. Benders decomposition for the uncapacitated multiple allocation hub location problem, *Computers & Operations Research* 35(4): 1047–1064. https://doi.org/10.1016/j.cor.2006.07.002

Dixit, V.; Seshadrinath, N.; Tiwari, M. K. 2016. Performance measures based optimization of supply chain network resilience: a NSGA-II + co-kriging approach, *Computers & Industrial Engineering* 93: 205–214. https://doi.org/10.1016/j.cie.2015.12.029

Drezner, Z. 1987. Heuristic solution methods for two location problems with unreliable facilities, *Journal of the Operational Research Society* 38(6): 509–514. https://doi.org/10.2307/2582764

Emecen Kara, E. G. 2016. Risk assessment in the Istanbul strait using Black sea MOU port state control inspections, *Sustainability* 8(4): 390. https://doi.org/10.3390/su8040390

Faghih-Roohi, S.; Ong, Y.-S.; Asian, S.; Zhang, A. N. 2016. Dynamic conditional value-at-risk model for routing and scheduling of hazardous material transportation networks, *Annals of Operations Research* 247(2): 715–734. https://doi.org/10.1007/s10479-015-1909-2

Fan, Y.; Liu, C. 2010. Solving stochastic transportation network protection problems using the progressive hedging-based method, *Networks and Spatial Economics* 10(2): 193–208. https://doi.org/10.1007/s11067-008-9062-y

Fan, Y.; Liu, C.; Lee, R.; Kiremidjian, A. S. 2010. Highway network retrofit under seismic hazard, *Journal of Infrastructure Systems* 16(3): 181–187. https://doi.org/10.1061/(asce)is.1943-555x.0000024

Filippi, C.; Mansini, R.; Stevanato, E. 2017. Mixed integer linear programming models for optimal crop selection, *Computers & Operations Research* 81: 26–39. https://doi.org/10.1016/j.cor.2016.12.004

Freund, R. M. 2004. *Benders' Decomposition Methods for Structured Optimization, Including Stochastic Optimization*. Massachusetts Institute of Technology, Cambridge, MA, US. 23 p.

Gotoh, J.-Y.; Takano, Y. 2007. Newsvendor solutions via conditional value-at-risk minimization, *European Journal of Operational Research* 179(1): 80–96. https://doi.org/10.1016/j.ejor.2006.03.022

Huang, Y.; Fan, Y.; Cheu, R. L. 2007. Optimal allocation of multiple emergency service resources for protection of critical transportation infrastructure, *Transportation Research Record: Journal of the Transportation Research Board* 2022: 1–8. https://doi.org/10.3141/2022-01

ISSConline. 2014. *A Wave of Strikes Springs the Ports All Over the World*. ISSConline, Xiamen, China. Available from Internet: https://www.issconline.com

John, A.; Paraskevadakis, D.; Bury, A.; Yang, Z.; Riahi, R.; Wang, J. 2014. An integrated fuzzy risk assessment for seaport operations, *Safety Science* 68: 180–194. https://doi.org/10.1016/j.ssci.2014.04.001

Jünger, M.; Liebling, T. M.; Naddef, D.; Nemhauser, G. L.; Pulleyblank, W. R.; Reinelt, G.; Wolsey, L. A. 2010. *50 Years of Integer Programming 1958–2008: from the Early Years to the State-of-the-Art.* Springer. 804 p. https://doi.org/10.1007/978-3-540-68279-0

Lei, X.; Shen, S.; Song, Y. 2018. Stochastic maximum flow interdiction problems under heterogeneous risk preferences, *Computers & Operations Research* 90: 97–109. https://doi.org/10.1016/j.cor.2017.09.004

Lewis, B. M.; Erera, A. L.; Nowak, M. A.; Chelsea, W. 2013. Managing inventory in global supply chains facing port-of-entry disruption risks, *Transportation Science* 47(2): 162–180. https://doi.org/10.1287/trsc.1120.0406

Li, Q.; Zeng, B.; Savachkin, A. 2013. Reliable facility location design under disruptions, *Computers & Operations Research* 40(4): 901–909. https://doi.org/10.1016/j.cor.2012.11.012

Li, X.; Ouyang, Y. 2010. A continuum approximation approach to reliable facility location design under correlated probabilistic disruptions, *Transportation Research Part B: Methodological* 44(4): 535–548. https://doi.org/10.1016/j.trb.2009.09.004

Liu, C.; Fan, Y.; Ordóñez, F. 2009. A two-stage stochastic programming model for transportation network protection, *Computers & Operations Research* 36(5): 1582–1590. https://doi.org/10.1016/j.cor.2008.03.001

Lu, J.; Gupte, A.; Huang, Y. 2018. A mean-risk mixed integer nonlinear program for transportation network protection, *European Journal of Operational Research* 265(1): 277–289. https://doi.org/10.1016/j.ejor.2017.07.025

Marufuzzaman, M.; Eksioglu, S. D.; Li, X.; Wang, J. 2014. Analyzing the impact of intermodal-related risk to the design and management of biofuel supply chain, *Transportation Research Part E: Logistics and Transportation Review* 69: 122–145. https://doi.org/10.1016/j.tre.2014.06.008

Miller-Hooks, E.; Chen, L.; Nair, R.; Mahmassani, H. S. 2009. Security and mobility of intermodal freight networks: evaluation framework for simulation and assignment, *Transportation Research Record: Journal of the Transportation Research Board* 2137: 109–117. https://doi.org/10.3141/2137-12

Miller-Hooks, E.; Zhang, X.; Faturechi, R. 2012. Measuring and maximizing resilience of freight transportation networks, *Computers & Operations Research* 39(7): 1633–1643. https://doi.org/10.1016/j.cor.2011.09.017

Mohaymany, A. S.; Pirnazar, N. 2007. Critical routes determination for emergency transportation network aftermath earthquake, in *2007 IEEE International Conference on Industrial Engineering and Engineering Management*, 2–5 December 2007, Singapore, 817–821. https://doi.org/10.1109/IEEM.2007.4419304

MoT. 2017. *Statistical Bulletin on Transportation Industry Development*. Ministry of Transport (MoT) of the People's Republic of China. Available from Internet: https://www.mot.gov.cn

Novati, M.; Achurra-Gonzalez, P.; Foulser-Piggott, R.; Bowman, G.; Bell, M. G. H.; Angeloudis, P. 2015. Modelling the effects of port disruptions: assessment of disaster impacts using a cost-based container flow assignment in liner shipping networks, in *Transportation Research Board 94th Annual Meeting*, 11–15 January 2015, Washington, DC, US, 1–16.

Noyan, N. 2012. Risk-averse two-stage stochastic programming with an application to disaster management, *Computers & Operations Research* 39(3): 541–559. https://doi.org/10.1016/j.cor.2011.03.017

Rockafellar, R. T.; Uryasev, S. 2000. Optimization of conditional value-at-risk, *Journal of Risk* 2(3): 21–41. https://doi.org/10.21314/jor.2000.038

Sawik, T. 2013a. Selection of optimal countermeasure portfolio in IT security planning, *Decision Support Systems* 55(1): 156–164. https://doi.org/10.1016/j.dss.2013.01.001

Sawik, T. 2013b. Selection of resilient supply portfolio under disruption risks, *Omega* 41(2): 259–269. https://doi.org/10.1016/j.omega.2012.05.003

Sawik, T. 2011. Selection of supply portfolio under disruption risks, *Omega* 39(2): 194–208. https://doi.org/10.1016/j.omega.2010.06.007

Shen, Z.-J. M.; Zhan, R. L.; Zhang, J. 2011. The reliable facility location problem: formulations, heuristics, and approximation algorithms, *INFORMS Journal on Computing* 23(3): 470–482. https://doi.org/10.1287/ijoc.1100.0414

Snyder, L. V.; Daskin, M. S. 2005. Reliability models for facility location: the expected failure cost case, *Transportation Science* 39(3): 400–416. https://doi.org/10.1287/trsc.1040.0107

Tan, Z.; Wang, G.; Ju, L.; Tan, Q.; Yang, W. 2017. Application of CVaR risk aversion approach in the dynamical scheduling optimization model for virtual power plant connected with wind-photovoltaic-energy storage system with uncertainties and demand response, *Energy* 124: 198–213. https://doi.org/10.1016/j.energy.2017.02.063

Uryasev, S. 2000. Conditional value-at-risk: optimization algorithms and applications, in *Proceedings of the IEEE/IAFE/INFORMS 2000 Conference on Computational Intelligence for Financial Engineering* (*CIFEr*), 26–28 March 2000, New York, NY, US, 49–57. https://doi.org/10.1109/cifer.2000.844598

Wang, X.; Meng, Q.; Miao, L. 2016. Delimiting port hinterlands based on intermodal network flows: Model and algorithm, *Transportation Research Part E: Logistics and Transportation Review* 88: 32–51. https://doi.org/10.1016/j.tre.2016.02.004

Xu, Q.; Zhou, Y.; Jiang, C.; Yu, K.; Niu, X. 2016. A large CVaR-based portfolio selection model with weight constraints, *Economic Modelling* 59: 436–447. https://doi.org/10.1016/j.econmod.2016.08.014

Yang, Z.; Ng, A. K. Y.; Wang, J. 2014. A new risk quantification approach in port facility security assessment, *Transportation Research Part A: Policy and Practice* 59: 72–90. https://doi.org/10.1016/j.tra.2013.10.025

Yu, G.; Haskell, W. B.; Liu, Y. 2017. Resilient facility location against the risk of disruptions, *Transportation Research Part B: Methodological* 104: 82–105. https://doi.org/10.1016/j.trb.2017.06.014